Journal of Biomechanics 124 (2021) 110546

Contents lists available at ScienceDirect

Journal of Biomechanics

journal homepage: www.elsevier.com/locate/jbiomech

Test-retest reliability of entire time-series data from hip, knee and ankle kinematics and kinetics during one-leg hops for distance: Analyses using integrated pointwise indices

Lina Schelin [a,*], Alessia Pini [b], Jonas L. Markström [c], Charlotte K. Häger [c]

[a] Department of Statistics, Umeå School of Business, Economics and Statistics, Umeå University, Samhällsvetarhuset, 901 87 Umeå, Sweden
[b] Department of Statistical Sciences, Università Cattolica del Sacro Cuore, Milan, Italy
[c] Department of Community Medicine and Rehabilitation, Physiotherapy, Umeå University, Umeå, Sweden

ARTICLE INFO

Keywords:
Biomechanics
Hop testing
Landing
Functional data
Motion analysis
Knee injury rehabilitation

ABSTRACT

Motion capture systems enable in-depth interpretations of human movements based on data from three-dimensional joint angles and moments. Such analyses carry important bearings for evaluation of movement control during for instance hop landings among sports-active individuals from a performance perspective but also in rehabilitation. Recent statistical development allows analysis of entire time-series of angle and moment during hops using functional data analysis, but the reliability of such multifaceted data is not established. We used integrated pointwise indices (intra-class correlation, ICC; standard error of measurement, SEM) to establish the test–retest reliability of three-dimensional hip, knee and ankle angle and moment curves during landings of one-leg hop for distance (OLHD) in 23 asymptomatic individuals aged 18–28. We contrasted these findings to reliability of discrete variables extracted at specific events (initial contact, peak value). We extended the calculations of ICC and SEM to handle unbalanced situations (varying number of repetitions) to include all available data. Hip and knee angle curves proved reliable with stable ICC curves throughout the landing, with integrated ICCs ≥ 0.71 for all planes except for knee internal/external rotation (ICC $= 0.57$). Hip and knee moment curves and ankle angle and moments were less reliable and less stable, particularly in the first $\sim$ 10–25% of the landing (integrated ICCs 0.44–0.57). Curve data were generally not in agreement with the results for discrete event data, thus advocating analysis of curve data which contains more information. To conclude, hip and knee angle curve data during OLHD landings can reliably be evaluated, while moment curves necessitate careful consideration.

1. Introduction

Motion capture is useful to evaluate joint angle and moment data during hop testing for sport-related purposes among both asymptomatic individuals and in rehabilitation of various clinical populations. Such time-series (curve) data are recorded during entire movements. However, commonly used statistical methods usually limit the analyses to specific discrete event-related variables, such as peak angles and moments during the landing phase. Recent development within the functional data analysis branch of statistics enables more advanced analysis of complete angle and moment curve data across the timeframe of interest. This approach provides a more complete representation of movement control than standard analyses of discrete event data since it includes a temporal aspect. Functional data analysis has been increasingly used to evaluate joint angle and moment curve data (see e.g., Hébert-Losier et al., 2015; 2018; Markström et al., 2019; Warmenhoven et al., 2019a; 2019b), but there is a need to evaluate test–retest reliability and purposive methods for this.

Hop tests are used to evaluate lower limb function and movement patterns in healthy and patient populations, but reliability evaluations have mainly targeted outcomes such as hop distance or height (e.g., Dingenen et al., 2019; Logerstedt et al., 2012). Test-retest reliability of curve data has nevertheless been established for the bilateral stop jump (Milner et al., 2011), drop vertical jump (Ford et al., 2007), single-leg drop (Myer et al., 2015), and single-leg cross drop (DiCesare et al., 2015). These studies used the coefficient of multiple correlation (CMC), which is a global measure of similarities between curves (McGinley et al., 2009). Their results generally showed moderate-to-excellent

* Corresponding author.
E-mail address: lina.schelin@umu.se (L. Schelin).

https://doi.org/10.1016/j.jbiomech.2021.110546
Accepted 31 May 2021
Available online 12 June 2021

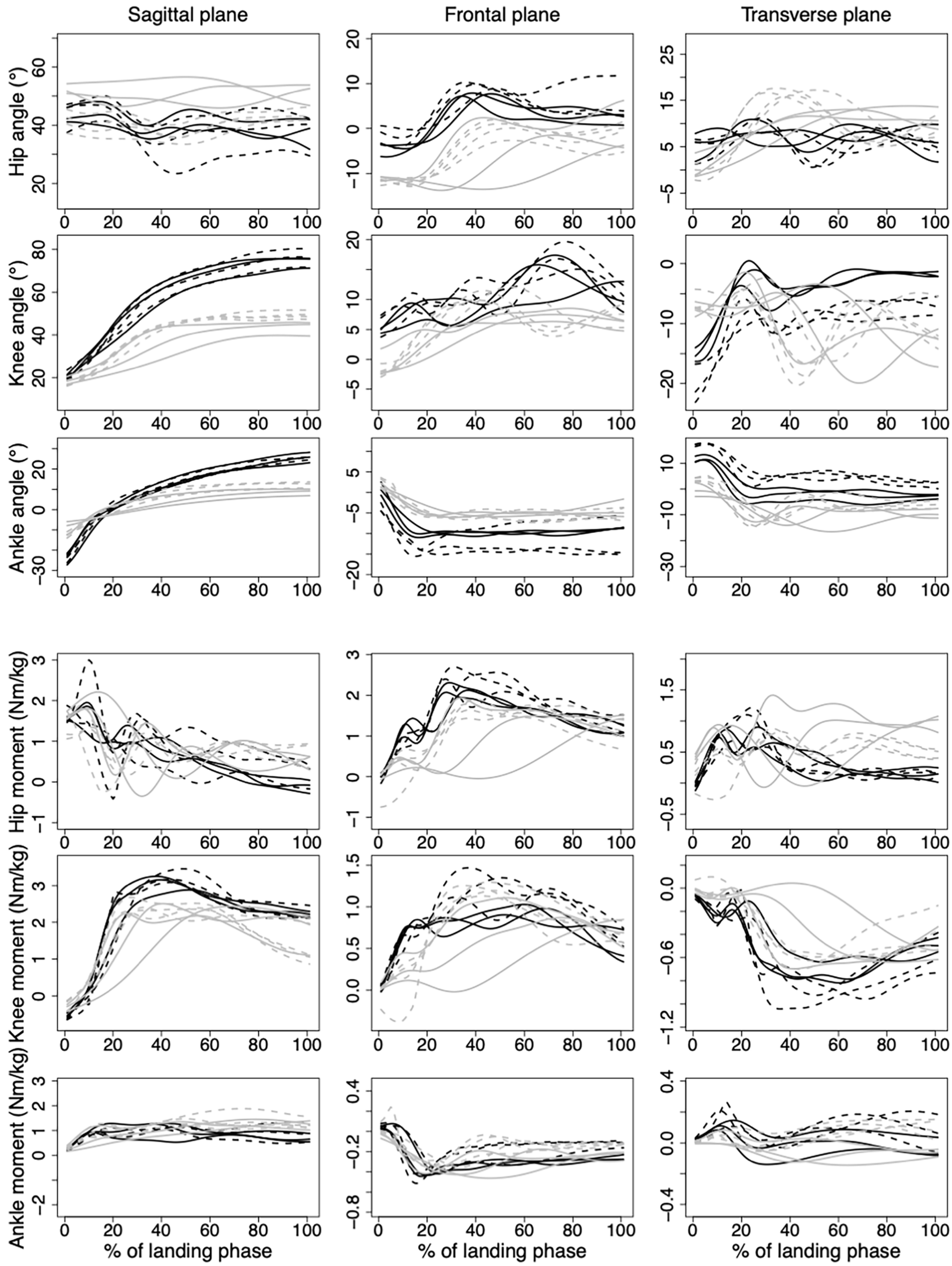

Fig. 1. Example of angle and moment curve data for two randomly chosen individuals during the landing phase of the one leg hop for distance. Solid lines indicate data from the first test session, while dashed lines refer to data from retest session. The two individuals are distinguished by black and gray color, respectively.

reliability for hip and knee angle (CMCs: 0.63–0.98) and moment (CMCs: 0.60–0.96) curves in all three planes. However, the CMC does not consider the inter-individual variation (Pini et al., 2019), which is an integrative part of reliability (Schwartz et al., 2004; Weir, 2005). An alternative and recently recommended method to evaluate reliability for curve data is to use *integrated pointwise indices,* including the intraclass correlation (ICC) and standard error of measurement (SEM) (Pini et al., 2019). These indices have previously been applied to lower limb joint angles during gait (Schwartz et al., 2004), and knee angles and moments during side-cutting (Sankey et al., 2015) in all three planes of motion. Both these studies report variation in inter-session errors over the phase of interest, with standard deviations for knee angles of $\sim 2^{\circ}$ during gait and ~ 2–5.5° during side-cutting, respectively, and ~ 5–32 Nm for the latter. Further evaluation of test–retest reliability of lower limb kinematic and kinetic curves during commonly used hop tests is warranted, particularly for specific phases of movement sequences.

We applied the integrated pointwise indices to evaluate the reliability of lower limb joint angle and moment curve data during the one-leg hop for distance (OLHD). The OLHD is the most common hop test in research and clinical rehabilitation (Hegedus et al., 2015). The OLHD has been used to evaluate differences in lower limb control between the dominant and non-dominant legs for healthy persons (van der Harst et al., 2007), injury risk screening among soccer players (Read et al., 2018), neuromuscular control among children with hypermobility (Junge et al., 2015), and consequences of anterior cruciate ligament (ACL) injury on lower limb function (King et al., 2018; Markström et al., 2020; Wren et al., 2018). Whereas maximal hop distance is considered a reliable outcome (Ageberg et al., 1998; Paterno and Greenberger, 1996), it might not detect deficits in knee function among ACL-reconstructed individuals (Kotsifaki et al., 2020). The movement pattern during OLDH as reflected by joint angle and moment curve data may be more sensitive but is more complicated to reliably evaluate given the multiple degrees of freedom and movement variability.

Our aim was to evaluate the test–retest reliability of hip, knee, and ankle joint angle and moment curve data using integrated pointwise indices during OLHD landings in asymptomatic individuals. A secondary aim was to contrast the reliability of curve data to that of traditional discrete event-specific values during the hop landing. Further, the calculations of ICC and SEM were extended to handle unbalanced situations (varying number of hop trials) to allow usage of all available data (details in supplementary material). We hypothesized that ICCs and SEMs would vary over time for the angle and moment curves although still reliable, but with poorer reliability for moments and particularly in the frontal and transverse planes early after impact (cf. Sankey et al., 2015). We also hypothesized that angle and moments curves would show equal reliability as the corresponding discrete event-related data.

2. Methods

2.1. Participants and study design

Twenty-three (two males) asymptomatic physically active (median 8 Tegner activity scale) persons (mean (SD): age 22.4 (3.2) years, body height 1.70 (0.08) m, body mass 63.5 (8.7) kg, body mass index 22.0 (2.1) kg/m^2) participated. Inclusion criteria were age 17–34 years and no neurological/musculoskeletal conditions. Participants were clinically examined before the first test session and interviewed regarding any injuries by an experienced physiotherapist. Two test sessions were performed with an identical protocol with a mean of 16.4 days apart (SD 6.6; range 7–30). A power analysis performed for a test–retest study analyzing side hop landings in the same study population indicated a need for 22 participants (Markström et al., 2021). We therefore considered 23 participants sufficient for the current study. All participants provided written informed consent and the study was approved by the Regional Ethical Review Board (Dnr. 2015/67–31).

2.2. Experimental procedure and instruments

The OLHD was performed barefoot with participants standing on one leg with arms behind their back, holding a 25 cm long rope with knots on each side. Instructions were to hop forward as far as possible, land on the same leg, control the landing and restore balance as quickly as possible. Participants landed on a (masked) force plate surrounded by walkway elements. To avoid fatigue, participants alternated between the right and left leg every trial. Successful trials required 2–3 s single-leg stance after landing without touching the ground with the contralateral foot or moving the ipsilateral foot to keep balance or letting go of the rope. One to two test trials were performed for familiarization before completing three to five hops on each leg.

Marker coordinates were captured at 240 Hz using an eight-camera motion capture system (Oqus®, Qualisys AB, Gothenburg, Sweden), synchronized with a Kistler force plate (model 9260AA, Kistler Instrument AG, Winterthur, Switzerland) that recorded force data at 1200 Hz. Fifty-six passive spherical markers were used to construct a six degree-of-freedom model (see supplementary material). A functional joint method calculated hip joint centers (Schwartz and Rozumalski, 2005), while the mid-point of markers on the lateral and medial femur epicondyles and malleoli defined knee and ankle joint centers, respectively. The same test leader applied all markers and instructed all participants.

2.3. Data processing

Qualisys Track Manager (v.2.2, Qualisys AB, Gothenburg, Sweden) and Visual3D (v.5.02.19, C-Motion Inc., Germantown, MD, USA) software tools were used to process data. Marker data were filtered with a critically damped digital filter with a cut-off frequency of 15 Hz to remove high-frequency noise prior to calculation of the dependent variables (Kristianslund et al., 2012; Roewer et al., 2014). Hip and knee joint angles were calculated using joint coordinate systems with the Cardan rotation sequence of XYZ (X, mediolateral axis; Y, anteroposterior axis; Z, longitudinal axis) (Cole et al., 1993). Hip and knee joint moments normalized to body mass were calculated with inverse dynamics using a Resultant Moments approach (Baltzopoulos, 2021), with coordinate systems resolved in the proximal segment coordinate system. External moments were expressed in this study, with flexion, adduction and internal rotation defined as positive. The segments' masses were calculated based on the proportions of Dempster (1955). Angle and moment data were filtered with a fourth-order bidirectional zero lag low-pass Butterworth digital filter with a cut-off frequency of 15 Hz.

Reliability for hip, knee, and ankle angle and moment data in sagittal, frontal, and transverse planes were analyzed during the landing phase defined between initial contact (ground reaction force > 20 N) to maximal knee flexion angle. All angle and moment curves were time-normalized, with initial contact at 0% and maximal knee flexion angle at 100%. The outcome variables for the univariate analyses were angles and moments at initial contact, and peak values for angles and moments of hip flexion, hip adduction, hip internal rotation, knee flexion, knee abduction, knee internal rotation, ankle dorsiflexion, ankle adduction, and ankle internal rotation. These are commonly evaluated following ACL injury (Bates et al., 2017; 2020; Frank et al., 2013; Hewett et al., 2005; Kiapour et al., 2016). Hop distance was also documented. Data from all successful trials (median 3, interquartile range 0, range 1–4, at test and retest for each participant) for the dominant leg (preferred leg to kick a ball) were used in the analyses. Test-retest data for two randomly chosen individuals are presented in Fig. 1.

2.4. Statistics

A challenge when analyzing demanding multi-joint hop tests is that the observed data are not always balanced, i.e., that not all individuals present an equal number of successful trials. The standard formulas to calculate ICCs and SEMs (McGraw and Wong, 1996; Weir, 2005) do not cover this situation. In the current study, we extend the usual calculations of ICC and SEM to a test–retest framework with an unbalanced case. These formulas (see appendix) were applied to analyze reliability and agreement for curve data with integrated pointwise indices using the ICC and SEM, respectively. The ICCs and SEMs were also supplemented at each time point by a 95% pointwise confidence interval (CI). In short, the ICC (type: absolute agreement) and SEM were calculated using variance components of an ANOVA (unbalanced design) based on a two-way mixed effect model without interactions, as previously recommended for test-retests (Trevethan, 2017). This methodology was also applied to the discrete data. The classification of ICCs according to Cicchetti (1994) was adapted for interpretation (poor < 0.4, $0.4 \leq$ fair $<$ 0.6, $0.6 \leq$ good ≤ 0.74, $0.74 <$ excellent).

The integrated pointwise index calculations include the following steps: Fix a point t of the domain D where curve data are observed, in our case OLHD landings. Compute a value of ICC and a corresponding confidence interval for each t. This results in a pointwise ICC function including pointwise confidence intervals. The integrated pointwise index, i.e., the global measure of reliability, can be obtained by integrating the ICC-function over D:

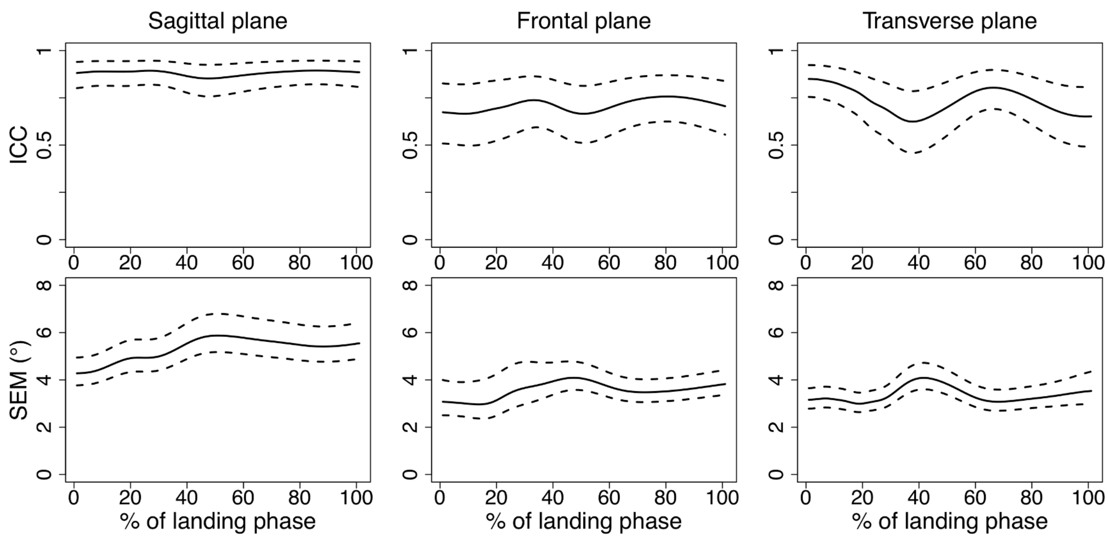

Fig. 2. Pointwise ICC (top row) and SEM (bottom row) including pointwise 95% confidence intervals for the hip angle during the landing phase (0–100%) for the sagittal, frontal and transverse planes. Data from all successful trials are included in the reliability analysis. See Table 1 for integrated indices. *Note.* The pointwise confidence intervals should be interpreted with care: for each point of the domain, the probability that the interval covers the true value is 95%, but the probability that the true curve is globally covered by the confidence band is not controlled.

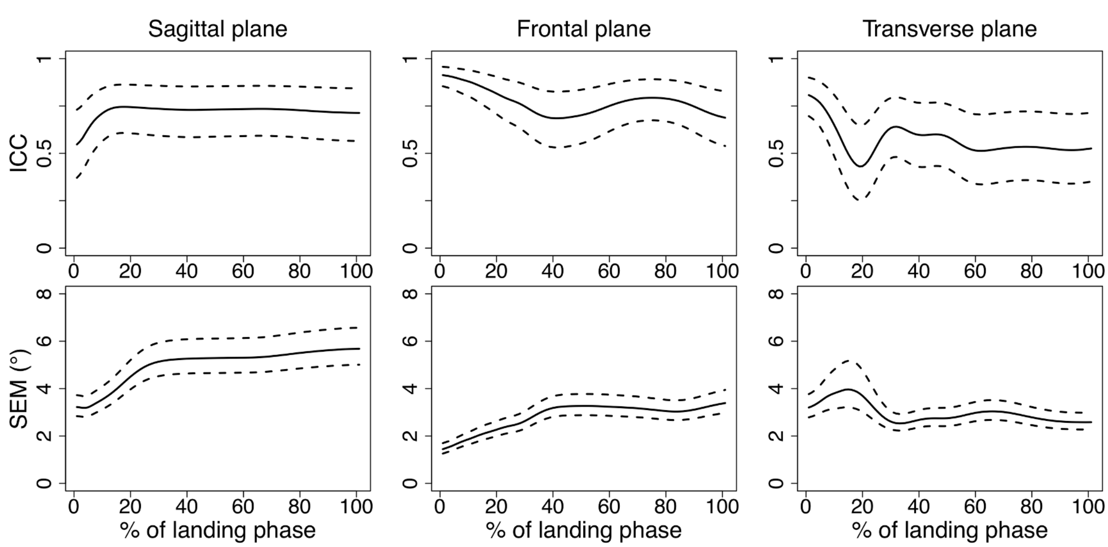

Fig. 3. Pointwise ICC (top row) and SEM (bottom row) including pointwise 95% confidence intervals for the knee angle during the landing phase (0–100%) for the sagittal, frontal and transverse planes. Data from all successful trials are included in the reliability analysis. See Table 1 for integrated indices. *Note.* The pointwise confidence intervals should be interpreted with care: for each point of the domain, the probability that the interval covers the true value is 95%, but the probability that the true curve is globally covered by the confidence band is not controlled.

$$\widehat{ICC} = \int_D \widehat{ICC}(t)dt$$

Similarly, a global measure of SEM can be obtained by integrating SEM(t) over D:

$$\widehat{SEM} = \int_D \widehat{SEM}(t)dt.$$

All analyses were performed using R (R Core Team, 2019). Free R-code is available for test–retest reliability analysis of curve data for immediate implementation (Pini et al., 2019), see also https://github.com/alessiapini/fdarely.

3. Results

Participants hopped a grand mean OLHD distance of 1.21 (0.23) m at test and 1.22 (0.22) m at retest. These data showed excellent reliability with an ICC of 0.89 (95% CI: 0.82, 0.95) and a SEM of 0.07 m (95% CI: 0.07–0.09 m).

3.1. Reliability of angle curves

Excellent reliability throughout the OLHD landing was shown for hip flexion; good-to-excellent reliability was shown for hip adduction/abduction and internal/external rotation, knee flexion and adduction/abduction, and ankle internal/external rotation; while fair-to-good reliability was shown for knee internal/external rotation, ankle plantar/dorsiflexion and adduction/abduction (the pointwise reliability of angle curves is displayed in Figs. 2–4 as a complement to the integrated indices in Table 1). The reliability for knee flexion increased from fair to excellent during the first ~ 15% of landing and stabilized afterward. In contrast, the reliability for knee internal/external rotation,

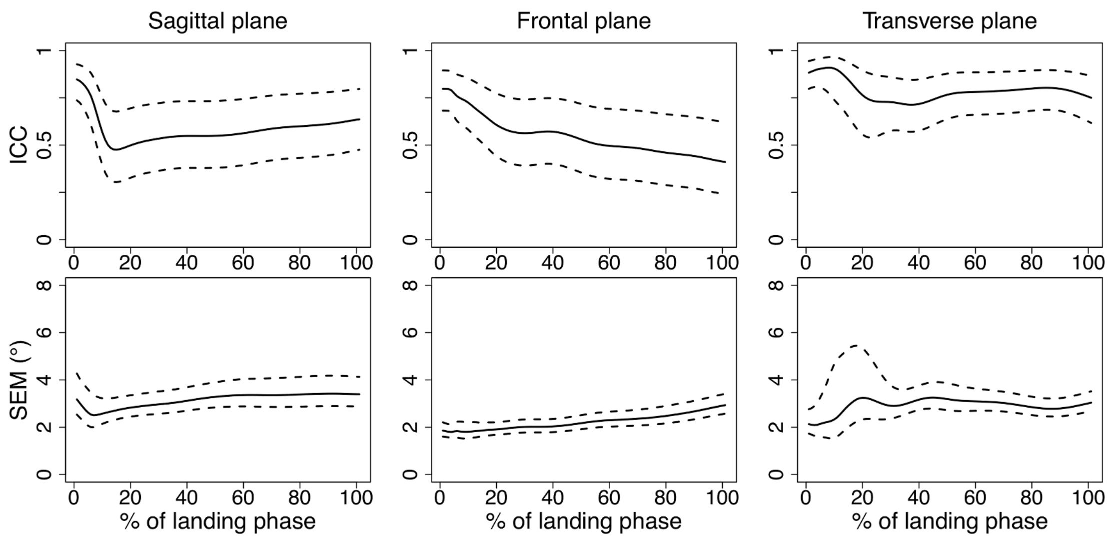

Fig. 4. Pointwise ICC (top row) and SEM (bottom row) including pointwise 95% confidence intervals for the ankle angle during the landing phase (0–100%) for the sagittal, frontal and transverse planes. Data from all successful trials are included in the reliability analysis. See Table 1 for integrated indices. *Note.* The pointwise confidence intervals should be interpreted with care: for each point of the domain, the probability that the interval covers the true value is 95%, but the probability that the true curve is globally covered by the confidence band is not controlled.

Table 1
Test-retest reliability of hip, knee and ankle angles and moments based on all available repetitions for curve data presented for the curve data using an integrated index, as well as for the discrete events at initial contact and at peak value. Confidence intervals are presented for discrete event ICCs and SEMs in parenthesis. For curve data reliability, point-wise confidence intervals are found in Figs. 2–7.

Outcomes for each motion plane		Integrated index		Initial contact		Peak value	
		ICC	SEM	ICC	SEM	ICC	SEM
Hip angles (°)	Sagittal	0.88	5.31	0.88 (0.80, 0.94)	4.28 (3.77, 4.95)	0.88 (0.80, 0.94)	5.52 (4.86, 6.38)
	Frontal	0.71	3.56	0.67 (0.51, 0.83)	3.08 (2.50, 4.00)	0.76 (0.63, 0.87)	3.36 (2.96, 3.89)
	Transverse	0.73	3.37	0.85 (0.75, 0.92)	3.16 (2.79, 3.65)	0.82 (0.72, 0.91)	2.95 (2.59, 3.42)
Knee angles (°)	Sagittal	0.72	5.01	0.55 (0.37, 0.73)	3.22 (2.84, 3.72)	0.71 (0.57, 0.84)	5.67 (5.00, 6.56)
	Frontal	0.77	2.83	0.91 (0.85, 0.96)	1.44 (1.26, 1.70)	0.79 (0.67, 0.89)	2.86 (2.47, 3.39)
	Transverse	0.57	2.98	0.81 (0.70, 0.90)	3.20 (2.79, 3.77)	0.56 (0.39, 0.74)	2.30 (2.03, 2.66)
Ankle angles (°)	Sagittal	0.58	3.15	0.85 (0.74, 0.93)	3.18 (2.53, 4.27)	0.62 (0.45, 0.78)	3.47 (2.93, 4.25)
	Frontal	0.55	2.22	0.80 (0.68, 0.90)	1.85 (1.60, 2.21)	0.79 (0.67, 0.89)	1.86 (1.62, 2.20)
	Transverse	0.79	2.92	0.88 (0.80, 0.94)	2.13 (1.73, 2.76)	0.89 (0.81, 0.95)	2.06 (1.64, 2.76)
Hip moments (Nm/kg)	Sagittal	0.57	0.35	0.36 (0.19, 0.57)	0.49 (0.43, 0.56)	0.63 (0.46, 0.79)	0.40 (0.35, 0.46)
	Frontal	0.44	0.33	0.33 (0.17, 0.55)	0.23 (0.20, 0.26)	0.63 (0.46, 0.79)	0.27 (0.24, 0.31)
	Transverse	0.51	0.22	0.25 (0.10, 0.47)	0.20 (0.18, 0.23)	0.72 (0.58, 0.85)	0.21 (0.18, 0.25)
Knee moments (Nm/kg)	Sagittal	0.56	0.37	0.27 (0.11, 0.49)	0.21 (0.19, 0.25)	0.39 (0.22, 0.60)	0.33 (0.29, 0.38)
	Frontal	0.54	0.25	0.23 (0.08, 0.45)	0.12 (0.11, 0.14)	0.61 (0.44, 0.77)	0.25 (0.22, 0.29)
	Transverse	0.45	0.14	−0.001 (−0.09, 0.16)	0.07 (0.06, 0.08)	0.07 (−0.04, 0.26)	0.10 (0.08, 0.11)
Ankle moments (Nm/kg)	Sagittal	0.43	0.29	0.19 (0.05, 0.41)	0.30 (0.26, 0.34)	0.36 (0.19, 0.58)	0.29 (0.26, 0.34)
	Frontal	0.52	0.09	0.12 (−0.01, 0.32)	0.07 (0.06, 0.08)	0.29 (0.13, 0.50)	0.07 (0.07, 0.09)
	Transverse	0.50	0.06	0.05 (−0.05, 0.24)	0.05 (0.05, 0.06)	0.45 (0.27, 0.65)	0.06 (0.05, 0.07)

ICC, intraclass correlation; SEM, standard error of measurement.

ankle plantar/dorsiflexion, and adduction/abduction decreased over the first ~ 15–30% of landing upon which it stabilized reaching fair reliability.

Regarding agreement, all SEM curves were relatively stable over the domain, apart from SEMs for hip and knee flexion that increased over time and fluctuated between ~ 3–6° (expected due to the simultaneous increases in angles during the landing; thus, did not result in lower ICC curves).

3.2. Reliability of moment curves

All moment curves showed substantial variation in reliability over the landing ranging from poor to good, with integrated ICCs of 0.43–0.57 (Table 1). The first ~ 10–25% of landing showed poor reliability for all moment curves. The reliability later increased and stabilized for hip flexion, knee flexion and adduction/abduction, and ankle adduction/abduction, and increased but varied for hip adduction/abduction and internal/external rotation, knee internal/external rotation, and ankle plantar/dorsiflexion and internal/external rotation (the pointwise reliability of moment curves is displayed in Figs. 4–6 as a complement to the integrated indices).

Concerning agreement, the SEM curves for hip and knee flexion varied for the first ~ 40% of landing with higher SEMs (up to ~ 0.55 Nm/kg) but stabilized afterward (~0.3 Nm/kg). The SEM curves for the remaining moments were relatively stable and had integrated SEMs of 0.06–0.33 Nm/kg.

3.3. Contrasts between reliability of curve data and discrete event-related data

Compared to ICCs at initial contact, the integrated ICC values were 0.11–0.45 higher for knee flexion angle and all moments, 0.12–0.27

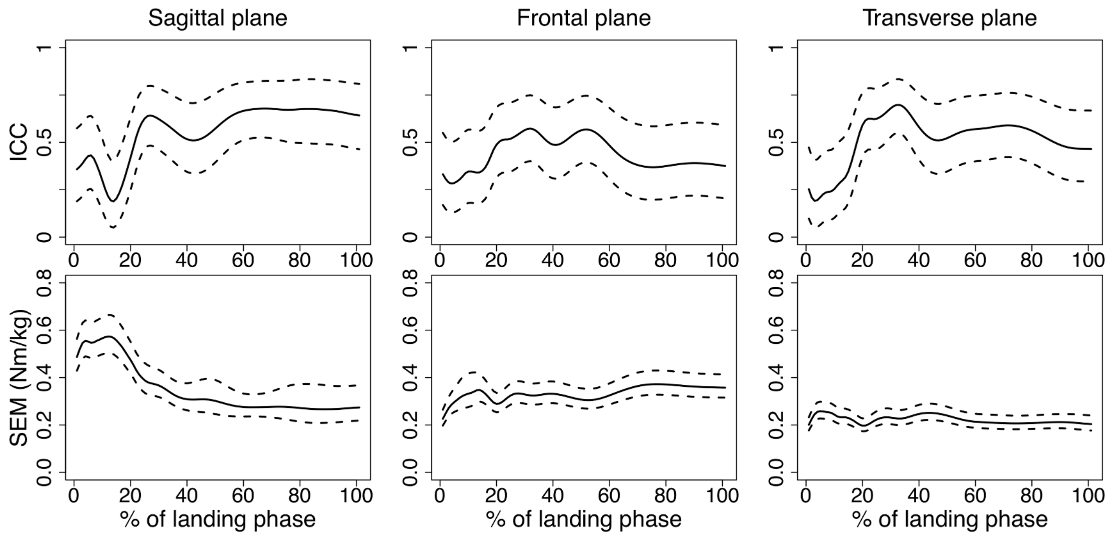

Fig. 5. Pointwise ICC (top row) and SEM (bottom row) including pointwise 95% confidence intervals for the hip moment during the landing phase (0–100%) for the sagittal, frontal and transverse planes. Data from all successful trials are included in the reliability analysis. See Table 1 for integrated indices. *Note.* The pointwise confidence intervals should be interpreted with care: for each point of the domain, the probability that the interval covers the true value is 95%, but the probability that the true curve is globally covered by the confidence band is not controlled.

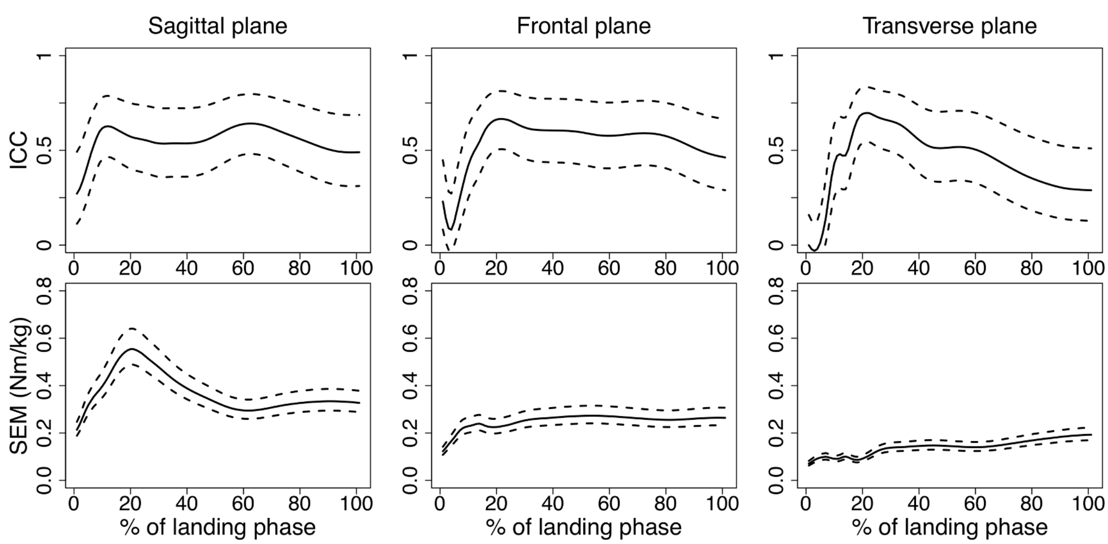

Fig. 6. Pointwise ICC (top row) and SEM (bottom row) including pointwise 95% confidence intervals for the knee moment during the landing phase (0–100%) for the sagittal, frontal and transverse planes. Data from all successful trials are included in the reliability analysis. See Table 1 for integrated indices. *Note.* The pointwise confidence intervals should be interpreted with care: for each point of the domain, the probability that the interval covers the true value is 95%, but the probability that the true curve is globally covered by the confidence band is not controlled.

lower for angles of hip and knee internal/external rotation, knee adduction/abduction, and ankle plantar/dorsiflexion and adduction/abduction, and were roughly similar for the remaining outcomes (0.00–0.09 difference). Compared to ICCs for peak values, the integrated ICCs were 0.17–0.37 higher for moments of knee flexion and internal/external rotation and ankle adduction/abduction, 0.10–0.24 lower for angles of ankle adduction/abduction and internal/external rotation and moments of hip adduction/abduction and internal/external rotation, and roughly similar for the remaining outcomes (0.00–0.09 difference).

Regarding agreement for angles, the integrated SEMs were ~ 1.4–1.8° higher than SEMs at initial contact for knee flexion and adduction/abduction, while the SEMs for all remaining angle outcomes (at initial contact and peak values) differed with less than ~ 1.0°. For moments, the integrated SEMs were 0.10–0.16 Nm/kg higher than hip and knee adduction/abduction and knee flexion, while the SEMs for all remaining moments differed with<0.07 Nm/kg.

4. Discussion

We evaluated the test–retest reliability of hip and knee joint angle and moment curves during OLHD landings in asymptomatic individuals and contrasted these findings to results from discrete data extracted at initial contact and peak values from the same data set. Angle curves generally displayed good-to-excellent reliability throughout the landing, except for knee internal/external rotation and ankle plantar/dorsiflexion and adduction/abduction. As hypothesized, moment curves in all planes were generally less reliable than angle curves, particularly in the first ~ 10–25%-time interval compared to the remaining part of the landing phase, despite hop lengths with small SEMs and excellent reliability. Further, the integrated indices for curve data were commonly not in agreement with the results for the discrete event data.

Our findings of lower ICCs for moments compared to angles are consistent with earlier results of hop and cutting tasks (Alenezi et al.,

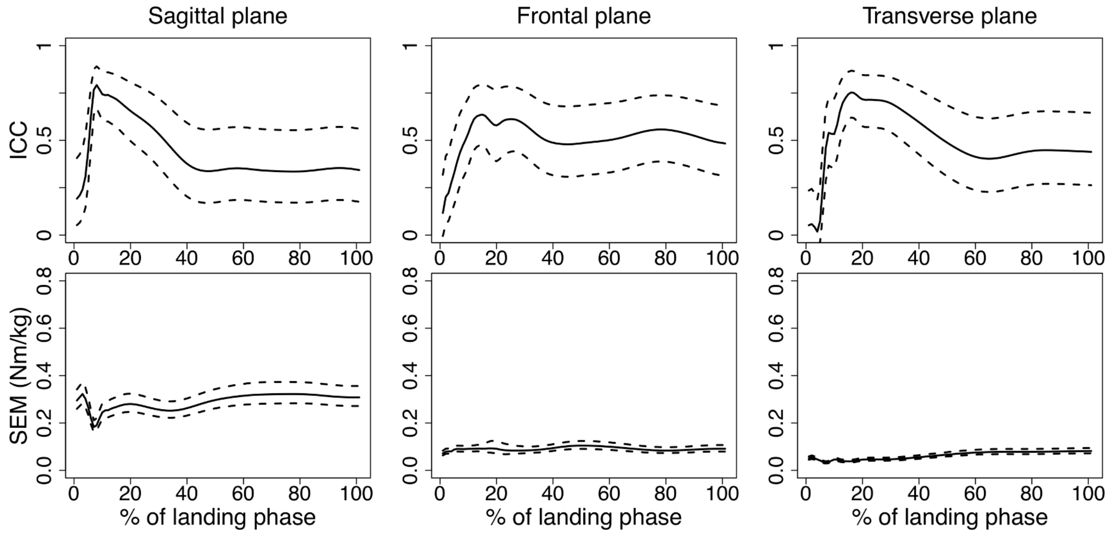

Fig. 7. Pointwise ICC (top row) and SEM (bottom row) including pointwise 95% confidence intervals for the ankle moment during the landing phase (0–100%) for the sagittal, frontal and transverse planes. Data from all successful trials are included in the reliability analysis. See Table 1 for integrated indices. *Note.* The pointwise confidence intervals should be interpreted with care: for each point of the domain, the probability that the interval covers the true value is 95%, but the probability that the true curve is globally covered by the confidence band is not controlled.

2016; Markström et al., 2021; Mok et al., 2018; Sankey et al., 2015). The poor-to-fair reliability for moments (both for the integrated and discrete values) suggests cautious use and interpretation. The poor reliability for moments immediately following landing constitutes a problem when assessing biomechanical risk factors for ACL injury/reinjury, considering ACL injury mechanics and strain (Bates et al., 2017; Frank et al., 2013; Imwalle et al., 2009; Kiapour et al., 2016), and that ACL injuries often occur within ~ 40 ms after impact (Koga et al., 2010; Krosshaug et al., 2007). Reliability for lower limb curve data later during the landing phase seems less problematic, while future research should assure reliability during the initial landing phase in ACL injury-prone tasks.

The poor reliability of joint moments initially during landing may be explained by the rapid increase in ground reaction force after initial contact and individual trial-to-trial differences in landing technique. The small joint moments at initial contact result in a low inter-individual variation, which (since related to intra-individual variation) affects the ICC calculation. These moments abruptly change after initial contact and are also influenced by landing technique, e.g., mid-flight whole-body and trunk rotation (Critchley et al., 2020), position of the foot (Houck, 2003) and trunk (Saito et al., 2020) at landing, and variation in postural control due to arm restriction (Chaudhari et al., 2005). A slight change in landing position at initial contact between trials for an individual, e.g., a few degrees variation of trunk rotation or foot plantar flexion, may influence how the force vector passes through the lower limb joints and result in dissimilar moments. While our standardization protocol (arms held behind the back) was implemented to avoid obscuring markers and emphasize lower limb control, it may have affected the trial-to-trial variation of the outcomes by hampering task completion. Moment data early after impact are also affected by the filtering process (Kristianslund et al., 2012; Roewer et al., 2014). A recent ISB recommendation paper highlighted that a similar frequency content of kinematic and kinetic data avoids moment artifacts not explained by the activity dynamics but may attenuate impact forces (Derrick et al., 2020). We chose not to filter the force data while filtering angle and moment data (the same 15 Hz cut-off). This was done to remove higher frequencies after applying the kinematic model, since it allowed some marker loss (we used > three markers per segment), potentially resulting in unwanted transients. The filtering procedure on moments early after landing should be carefully considered.

The higher reliability for angle curves than moment curves promotes the former when assessing movement patterns, e.g., when evaluating ACL injury risk related to both knee abduction angle at initial contact (Bates et al., 2020) and peak knee abduction moment (Hewett et al., 2005) during drop jump landings. While the OLHD is a different task and knee abduction angles may not be as pronounced, the knee joint contributes with 65% of work absorption of the lower limb joints during landing, compared to 34% for the one-leg vertical hop (Kotsifaki et al., 2021). Analyses of joint angle curves during OLHD landings should be considered in evaluation of lower limb function among healthy and patient populations. Collecting kinematic data also has lower technical demands than collecting moment data. A few markers and two portable computer devices are sufficient to calculate simple angle variables and enable data collection outside the laboratory (Peebles et al., 2021).

We adopted the commonly used ICC classification according to Cicchetti (1994). Notably, other ICC thresholds exist (e.g., Koo and Li, 2016) and can be applied to the values reported in Table 2. However, we did not provide SEM thresholds due to the lack of such estimates. SEM sizes need nevertheless to be related to the range of the data. For clinical purposes, it would be interesting to compare SEMs with minimal clinically important differences. However, as pointed out in a systematic review by Kotsifaki et al. (2020), those are seldom known in these task contexts.

Curve data provides reliability outcomes comparable to and in excess of commonly used discrete event variables and enables a greater understanding of movement control during different landing phases. Our results expand on and provide an alternative methodology compared to reports of reliability of curve data from other types of hops using the criticized measure CMC (DiCesare et al., 2015; Ford et al., 2007; Milner et al., 2011; Myer et al., 2015). The CMC does not incorporate the inter-individual variation (Pini et al., 2019), and it may also be undefined for a small range of motion (Chia and Sangeux, 2017; Røislien et al., 2012). Similar to the analysis of lower limb joint angles during gait (Schwartz et al., 2004) and knee angles and moments during side-cutting (Sankey et al., 2015), we found that ICCs and SEMs of angles and moments varied over the observed domain (Figs. 2–7). Hence, the integrated ICC and SEM cannot always be assumed to represent the entire curve's characteristics adequately. The curve data are therefore favored over discrete event-related outcomes. For reliability investigations of curve data, we recommend visualizing the pointwise ICCs and SEMs with confidence intervals along with the integrated indices to evaluate if the curve data are stable enough to use the integrated indices. However, the pointwise confidence intervals should be interpreted with care since, for each point of the domain, the probability that the interval covers the true value is 95%, but the probability that the true curve is globally covered by the confidence bands is not controlled for. This distinction is emphasized to avoid unnecessary misinterpretation of the results. Future research should develop methods for simultaneous confidence bands (instead of pointwise intervals) and confidence intervals for the integrated indices. Confidence interval methods for ICC are compared in Ionan et al. (2014). These intervals, or intervals based on bootstrap techniques, might be suitable after verifying their properties.

A novelty of our analysis is the extension of the definitions of ICC and SEM to the case of unbalanced designs with different numbers of trials. There are many reasons for different trial numbers across or within individuals, or between test and retest. In our study, the reason was the difficulty of achieving successful trials among a limited number of executed trials (to avoid the onset of fatigue considering that OLHD is a maximal-effort test). Including all available trials in the analysis reduces the estimate's variance, leading to narrower confidence intervals for ICCs and SEMs, and thus a more precise estimate of the two quantities. Caution should be taken if the number of repetitions varies substantially depending on the performance ability, risking biased estimates, or if the unbalance is large.

As for limitations, we analyzed asymptomatic individuals, and further research is warranted on individuals with lower limb injuries for clinical implications. We included more females than males, which could bias the results. However, this would seem less problematic for reliability purposes, assuming that the variation in test–retest performance is similar between sexes. Our data for males were within the range of values reported for females, and we found similar results of ICCs and SEMs when including only females. Further, the OLHD testing performed barefoot with arms restricted may also have affected our results despite the familiarization trials. While we found no significant improvement in hop distance from test to retest (mean 0.01 (SD 0.10) m difference) nor across trials within the test sessions, a more thorough familiarization protocol with a pre-testing session may nevertheless be advantageous to control for such bias and thus improve the reliability. Variation in marker placement to approximate knee and ankle joint centers (we used a functional joint method for the hip) between test and retest may also reduce reliability. Functional joint methods to approximate knee and ankle joint centers may cause smaller inter-session variance (Schache et al., 2006), smaller inter-assessor variance and less effects of high body mass (Meng et al., 2020), while avoiding over- and underestimating ankle torques in different planes of motion (Sado et al., 2021). However, our participants were physically active and relatively lean (mean body mass index of 22.0 (SD 2.1) kg/m^2), and the same person applied and controlled markers on all participants at both test sessions.

In summary, curve data of hip and knee joint angles in all three planes of motion, except for knee internal/external rotation angle, proved reliable and stable over OLHD landings across test sessions using integrated pointwise indices (ICC, SEM). The corresponding moments, and also angle and moment curves for the ankle, were less reliable, particularly early after landing. Similar concerns applied to discrete moment data at initial contact for hip, knee, and ankle joints in all planes, while peak values for the hip joint in all planes and the knee joint in the frontal plane were reliable. Further, the integrated indices were mostly higher than or similar to the corresponding discrete event data at initial contact and relatively similar to peak value data. Therefore, we recommend using integrated indices combined with pointwise indices with confidence intervals for a more comprehensive evaluation of curve data. Curve analysis of OLHD landings is recommended for hip and knee angles, while moments for the hip, knee, and ankle early after landing should be handled with caution.

Declaration of Competing Interest

The authors declare that they have no known competing financial interests or personal relationships that could have appeared to influence the work reported in this paper.

Acknowledgements

The study was funded by the Swedish Scientific Research Council (Häger Grant No. 2017-00892, Schelin 2016-02763); Region Västerbotten (Häger Grant No. ALF VLL548501, VLL838421 and Strategic funding VLL-358901; Project No. 7002795), the Swedish Scientific Research Council for Sports Science (Häger Grant No. Dnr CIF 2017/8 P2018-0104), and King Gustaf V and Queen Victoria's Foundation of Freemasons (Häger 2020). The funders had no involvement in any part of the study. Andrew Strong, PhD, is gratefully acknowledged for assisting in the data collection, and we also acknowledge the significant contribution of the anonymous reviewers.

Data statement

The data can be available on request for scientific purposes not violating Swedish legislation, guaranteeing individual confidentiality. Umeå University is responsible for the personal data and for data requests, interested researchers may contact the principal investigator Professor Charlotte Häger, charlotte.hager@umu.se.

Appendix A. Details on statistical methodology

In this work we extend the usual concepts of ICC and SEM to a test–retest framework for the unbalanced case, i.e., we do not assume that the number of trials for each test session and each individual, is the same. Specifically, fix a point t of the domain D. Let $Y_{gij}(t)$ be the value at point $t \in D$ of the curve of individual $i = 1, \cdots, n$ measured at test session $g = 1, \cdots, G$ in the repetition/trial $j = 1, \cdots, J_{gi}$. Note that we assume the possibility of observing a different number of repetitions J_{gi} for each individual in each test session. Denote as $J_{..} = \sum_{g=1}^{G}\sum_{i=1}^{n} J_{gi}$ the total number of data that we observe. We assume that the curve $Y_{gij}(t)$ follow the two-way anova model (without interaction):

$$Y_{gij}(t) = \mu(t) + \tau_i(t) + \gamma_g(t) + \varepsilon_{gij}(t),$$

where $\mu(t)$ is the mean value common to all subjects and test sessions, $\tau_i(t)$ is the subject effect, $\gamma_g(t)$ is the test session effect and $\varepsilon_{gij}(t)$ are independent and identically distributed (i.i.d.) error terms. We assume that subjects' and test sessions' effects are random. In particular, $\tau_i(t)$ for $i = 1, \cdots, n$ are i.i.d. (with respect to individuals) normally distributed random variables with zero mean and variance $\sigma_S^2(t)$, and $\gamma_g(t)$ for $g = 1, \cdots, G$ are i.i.d. (with respect to test sessions) normally distributed random variables with zero mean and variance $\sigma_T^2(t)$. We also assume that the errors $\varepsilon_{gij}(t)$ are i.i.d. (with respect to test sessions, individuals, and trials) normally distributed random variables with zero mean and variance $\sigma_E^2(t)$, and that for all t, all terms are independent between each other.

Using the specified model, it is possible to decompose the total sum of squares $SS_{TOT}(t)$ of data $Y_{gij}(t)$ into three different terms:

$$SS_{TOT}(t) = SS_S(t) + SS_T(t) + SS_E(t),$$

where $SS_S(t)$ indicates the amount of variability between different subjects, $SS_T(t)$ indicates the amount of variability of the data between test sessions, and $SS_E(t)$ indicates the residual variability. Table A1 reports the ANOVA table for the case in exam, indicating the sum of squares, corresponding degrees of freedom and mean squares.

The last column of Table A1 reports the expected mean squares, that were obtained by Eze and Chigbu (2012) in the case of unbalanced designs, where:

$$k_S = \frac{N - N^{-1}\sum_{i=1}^{n} J_{\cdot i}^2}{n-1} \qquad k_T = \frac{N - N^{-1}\sum_{g=1}^{G} J_{g\cdot}^2}{G-1}$$

and where

$$N = J_{\cdot\cdot} = \sum_{g=1}^{G}\sum_{i=1}^{n} J_{gi} \qquad J_{\cdot i} = \sum_{g=1}^{G} J_{gi} \qquad J_{g\cdot} = \sum_{i=1}^{n} J_{gi}$$

$$\overline{Y}_{\dots}(t) = \frac{1}{J_{\cdot\cdot}}\sum_{g=1}^{G}\sum_{i=1}^{n}\sum_{j=1}^{J_{gi}} Y_{gij}(t)$$

$$\overline{Y}_{\cdot i\cdot}(t) = \frac{1}{J_{\cdot i}}\sum_{g=1}^{G}\sum_{j=1}^{J_{gi}} Y_{gij}(t) \qquad \overline{Y}_{g\cdot\cdot}(t) = \frac{1}{J_{g\cdot}}\sum_{i=1}^{n}\sum_{j=1}^{J_{gi}} Y_{gij}(t).$$

In the following we show how to derive ICC and SEM based on the terms of variance decomposition of Table A1.

Intraclass correlation coefficient

The ICC can be estimated considering the values of expected mean squares (see Fleiss and Shrout (1978) for the classical case with $J_{gi} = 1$). In detail, the theoretical value of the ICC is:

$$ICC(t) = \frac{\sigma_S^2(t)}{\sigma_S^2(t) + \sigma_T^2(t) + \sigma_E^2(t)}.$$

The latter formula corresponds to ICC(k,1) in the modern notation. A consistent estimate of the ICC is obtained with the ratio of unbiased estimates of the numerator and denominator of the previous expression:

$$\widehat{ICC}(t) = \frac{k_T(MS_S(t) - MS_E(t))}{k_S MS_T(t) + k_T MS_S(t) + (k_S k_T - k_S - k_T)MS_E(t)}.$$

Observe that the theoretical value of the ICC is always positive. The estimate however might attain negative values. When this happens in practice, it only implies that the true ICC value is really low.

In addition to the estimate, it is possible to provide at each time point t a confidence interval for the ICC. Fleiss and Shrout (1978) derive confidence intervals for the ICC in the case $J_{gi} = 1$. In this work we derive the general formulation of confidence interval for the unbalanced design that we are addressing, based on Table A1 (the modified ANOVA table). Specifically, consider the quantity

$$V(t) = \frac{1}{k_T(1 - ICC(t))}\{k_S ICC(t) MS_T(t) + [k_T(1 + (k_S - 1)ICC(t)) - k_S ICC(t)]MS_E(t)\}$$

It is possible to show that the expected values of $V(t)$ and of $MS_S(t)$ coincide for all t. In addition, by simple algebra, we have that:

$$V(t) = a(t)MS_T(t) + b(t)MS_E(t),$$

where

$$a(t) = \frac{k_S\widehat{ICC}(t)}{k_T\left(1 - \widehat{ICC}(t)\right)}$$

$$b(t) = 1 + \frac{\widehat{ICC}(t)k_S(k_T - 1)}{k_T\left(1 - \widehat{ICC}(t)\right)}.$$

Following Satterthwaite (1946), we have that $V(t)$ properly rescaled follows approximately a chi-square distribution whose approximate degrees of freedom are given by:

Table A1

Two-way ANOVA table with replicates/repetitions in the case of unbalanced designs.

Factor	df	SS	MS	EMS
Subject	$n-1$	$SS_S(t) = \sum_{i=1}^{n}\left[\left(\overline{Y}_{\cdot i\cdot}(t) - \overline{Y}_{\dots}(t)\right)^2\sum_{g=1}^{G} J_{gi}\right]$	$MS_S(t) = \frac{SS_S(t)}{n-1}$	$\sigma_E^2(t) + k_S\sigma_S^2(t)$
Test Session	$G-1$	$SS_T(t) = \sum_{g=1}^{G}\left[\left(\overline{Y}_{g\cdot\cdot}(t) - \overline{Y}_{\dots}(t)\right)^2\sum_{i=1}^{n} J_{gi}\right]$	$MS_T = \frac{SS_T(t)}{G-1}$	$\sigma_E^2(t) + k_T\sigma_T^2(t)$
Error	$J_{\cdot\cdot} - n - G + 1$	$SS_E(t) = \sum_{g=1}^{G}\sum_{i=1}^{n}\sum_{j=1}^{J_{gi}}\left[\left(Y_{gij}(t) - \overline{Y}_{\cdot i\cdot}(t) - \overline{Y}_{g\cdot\cdot}(t) + \overline{Y}_{\dots}(t)\right)^2\right]$	$MS_E = \frac{SS_E}{J_{\cdot\cdot} - n - G + 1}$	σ_E^2

$$\nu(t) = \frac{(a(t)MS_T(t) + b(t)MS_E(t))^2}{\frac{(a(t)MS_T(t))^2}{G-1} + \frac{(b(t)MS_E(t))^2}{J_{..}-n-G+1}}.$$

Finally, note that $V(t)$ and of $MS_S(t)$ have the same expected value, and they are mutually independent. Consequently, their ratio is approximately distributed as:

$$\frac{MS_S(t)}{V(t)} \approx F_{n-1,\nu(t)}.$$

For the lower bound of a confidence interval on the ICC, note that with probability $1-\alpha/2$,

$$\frac{MS_S(t)}{V(t)} \le F^{\alpha/2}_{\nu(t),n-1}.$$

Rearranging the terms in the latter equation, we obtain the lower bound of the α-level confidence interval:

$$ICC(t) \ge \frac{k_T\left(MS_S(t) - F^{\alpha/2}_{n-1,\nu t)}MS_E(t)\right)}{k_T MS_S(t) + F^{\alpha/2}_{n-1,\nu(t)}(k_S MS_T(t) + (k_T k_S - k_T - k_S)MS_E(t))}.$$

Similarly, we obtain the upper bound of the confidence interval:

$$ICC(t) \le \frac{k_T\left(F^{\alpha/2}_{\nu(t),n-1}MS_S(t) - MS_E(t)\right)}{k_S MS_T(t) + (k_T k_S - k_T - k_S)MS_E(t) + k_T F^{\alpha/2}_{\nu(t),n-1}MS_S(t)}.$$

It should be noticed that, for the balanced case, the upper and lower bounds for the ICC (at each point t) exactly correspond to the formulas for $ICC(A,1)$ in Table 7 on page 41 in McGraw and Wong (1996).

A different value of ICC and of ICC confidence interval is computed for each time point t, providing a pointwise ICC function. Such function is useful to assess whether data can be considered reliable along the whole domain, or if there is a high variation of reliability along the domain. The integrated pointwise index, i.e., the global measure of reliability, can be obtained by integrating the ICC function over the domain D:

$$\widehat{ICC} = \int_D \widehat{ICC}(t)\mathrm{d}t.$$

Standard error of measurement

Accompanying the ICCs is the standard error of measurement (SEM) to provide an estimate of agreement. SEM quantifies the expected trial-to-trial noise in the data, i.e., how much the data measured for the same individual are expected to vary between the G test sessions. Unlike the ICC, the SEM is an absolute quantity, i.e., its value depends on the unit of measurement of the data. As discussed for instance by Weir (2005), there exist different versions of the SEM. In this work, to be consistent with the ICC, we consider the estimate of the SEM starting by the mean square errors terms in Table A1. Specifically, since we want to quantify the variability of the measurements across trials and test sessions, the theoretical value of the SEM at point t is:

$$SEM(t) = \sqrt{\sigma_T^2 + \sigma_E^2}$$

In the unbalanced design considered in this paper, an unbiased estimate of the squared value of the pointwise SEM is given by

$$\widehat{SEM}^2(t) = \frac{MS_T(t) + (k_T - 1)MS_E(t)}{k_T} = cMS_T + dMS_E$$

where

$$c = \frac{1}{k_T}, \qquad d = \frac{k_T - 1}{k_T}.$$

Following the approximation given by Satterthwaite (1946), we have

$$\eta(t)\frac{\widehat{SEM}^2(t)}{SEM^2(t)} \approx \chi^2_{\eta(t)},$$

where:

$$\eta(t) = \frac{[cMS_T(t) + dMS_E(t)]^2}{\frac{[cMS_T(t)]^2}{G-1} + \frac{[dMS_E(t)]^2}{J_{..}-n-G+1}}.$$

This approximate distribution can be used to compute the following approximate pointwise confidence interval for the SEM:

$$\frac{\eta(t)\widehat{SEM}^2(t)}{\chi^2_{\eta(t),\alpha/2}} \le SEM^2(t) \le \frac{\eta(t)\widehat{SEM}^2(t)}{\chi^2_{\eta(t),1-\alpha/2}}$$

$$\sqrt{\frac{\eta(t)\widehat{SEM}^2(t)}{\chi^2_{\eta(t),\alpha/2}}} \leq SEM(t) \leq \sqrt{\frac{\eta(t)\widehat{SEM}^2(t)}{\chi^2_{\eta(t),1-\alpha/2}}}.$$

Finally, a global measure of SEM can be obtained by integrating $SEM(t)$ over the domain:

$$\widehat{SEM} = \int_D \widehat{SEM}(t)\mathrm{d}t.$$

Appendix B. Supplementary material

Supplementary data to this article can be found online at https://doi.org/10.1016/j.jbiomech.2021.110546.

References

Ageberg, E., Zätterström, R., Moritz, U., 1998. Stabilometry and one-leg hop test have high test-retest reliability. Scand. J. Med. Sci. Sports 8, 198–202.
Alenezi, F., Herrington, L., Jones, P., Jones, R., 2016. How reliable are lower limb biomechanical variables during running and cutting tasks. J. Electromyog. Kinesiol. 30, 137–142.
Baltzopoulos, V., 2021. Inverse dynamics, joint reaction forces and loading in the musculoskeletal system: guidelines for correct mechanical terms and recommendations for accurate reporting of results. Sports Biomech. https://doi.org/10.1080/14763141.2020.1841826.
Bates, N.A., Myer, G.D., Hale, R.F., Schilaty, N.D., Hewett, T.E., 2020. Prospective Frontal Plane Angles Used to Predict ACL Strain and Identify Those at High Risk for Sports-Related ACL Injury. Orthop J Sports Med. 13;8:2325967120957646.
Bates, N.A., Nesbitt, R.J., Shearn, J.T., Myer, G.D., Hewett, T.E., 2017. Knee abduction affects greater magnitude of change in ACL and MCL strains than matched internal tibial rotation in vitro. Clin. Orthop. Relat. Res. 475, 2385–2396.
Chaudhari, A.M., Hearn, B.K., Andriacchi, T.P., 2005. Sport-dependent variations in arm position during single-limb landing influence knee loading: implications for anterior cruciate ligament injury. Am. J. Sports Med. 33 (6), 824–830.
Chia, K., Sangeux, M., 2017. Quantifying sources of variability in gait analysis. Gait Posture 56, 68–75.
Cicchetti, D.V., 1994. Guidelines, criteria, and rules of thumb for evaluating normed and standardized assessment instruments in psychology. Psychol. Methods 6 (4), 284–290.
Cole, G.K., Nigg, B.M., Ronsky, J.L., Yeadon, M.R., 1993. Application of the joint coordinate system to three-dimensional joint attitude and movement representation: a standardization proposal. J. Biomech. Eng. 115, 344–349.
Critchley, M.L., Davis, D.J., Keener, M.M., Layer, J.S., Wilson, M.A., Zhu, Q., Dai, B., 2020. The effects of mid-flight whole-body and trunk rotation on landing mechanics: implications for anterior cruciate ligament injuries. Sports Biomech. 19 (4), 421–437.
Derrick, T.R., van den Bogert, A.J., Cereatti, A., Dumas, R., Fantozzi, S., Leardini, A., 2020. ISB recommendations on the reporting of intersegmental forces and moments during human motion analysis. J Biomech. 99, 109533. https://doi.org/10.1016/j.jbiomech.2019.109533.
DiCesare, C.A., Bates, N.A., Barber Foss, K.D., Thomas, S.M., Wordeman, S.C., Sugimoto, D., Roewer, B.D., Medina McKeon, J.M., Di Stasi, S., Noehren, B.W., Ford, K.R., Kiefer, A.W., Hewett, T.E., Myer, G.D., 2015. Reliability of 3-dimensional measures of single-leg cross drop landing across 3 different institutions: implications for multicenter biomechanical and epidemiological research on ACL injury prevention. Orthop. J. Sports Med. 3 (12), 1–9. https://doi.org/10.1177/2325967115617905.
Dingenen, B., Truijen, J., Bellemans, J., Gokeler, A., 2019. Test–retest reliability and discriminative ability of forward, medial and rotational single-leg hop tests. Knee 26 (5), 978–987.
Dempster, W.T., 1955. The anthropometry of body action. Ann. N.Y. Acad. Sci. 63 (4), 559–585.
Eze, F., Chigbu, P., 2012. Unbalanced two-way random model with integer-value degrees of freedom. J. Nat. Sci. Res. 2, 100–107.
Fleiss, J.L., Shrout, P.E., 1978. Approximate interval estimation for a certain intraclass correlation coefficient. Psychometrika 43 (2), 259–262.
Ford, K.R., Myer, G.D., Hewett, T.E., 2007. Reliability of landing 3D motion analysis: implications for longitudinal analyses. Med. Sci. Sports Exerc. 39, 2021–2028.
Frank, B., Bell, D.R., Norcross, M.F., Blackburn, J.T., Goerger, B.M., Padua, D.A., 2013. Trunk and hip biomechanics influence anterior cruciate loading mechanisms in physically active participants. Am. J. Sports Med. 41 (11), 2676–2683.
Hébert-Losier, K., Pini, A., Vantini, S., Strandberg, J., Abramowicz, K., Schelin, L., Häger, C.K., 2015. One-leg hop kinematics 20 years following anterior cruciate ligament rupture: Data revisited using functional data analysis. Clin. Biomech. 30 (10), 1153–1161.
Hébert-Losier, K., Schelin, L., Tengman, E., Strong, A., Häger, C.K., 2018. Curve analyses reveal altered knee, hip, and trunk kinematics during drop–jumps long after anterior cruciate ligament rupture. Knee 25 (2), 226–239.
Hegedus, E.J., McDonough, S., Bleakley, C., Cook, C.E., Baxter, G.D., 2015. Clinician-friendly lower extremity physical performance measures in athletes: a systematic review of measurement properties and correlation with injury, part 1. The tests for knee function including the hop tests. Br. J. Sports Med. 49 (10), 642–648.
Hewett, T.E., Myer, G.D., Ford, K.R., Heidt, R.S., Colosimo, A.J., McLean, S.G., van den Bogert, A.J., Paterno, M.V., Succop, P., 2005. Biomechanical measures of neuromuscular control and valgus loading of the knee predict anterior cruciate ligament injury risk in female athletes: a prospective study. Am. J. Sports Med. 33 (4), 492–501.
Houck, J., 2003. Muscle activation patterns of selected lower extremity muscles during stepping and cutting tasks. J. Electromyog. Kinesiol. 13 (6), 545–554.
Imwalle, L.E., Myer, G.D., Ford, K.R., Hewett, T.E., 2009. Relationship between hip and knee kinematics in athletic women during cutting maneuvers: a possible link to noncontact anterior cruciate ligament injury and prevention. J. Strength Cond. Res. 23, 2223–2230.
Ionan, A.C., Polley, M.Y.C., McShane, L.M., Dobbin, K.K., 2014. Comparison of confidence interval methods for an intra-class correlation coefficient (ICC). BMC Med Res Methodol. 14, 1–11.
Junge, T., Wedderkopp, N., Thorlund, J.B., Søgaard, K., Juul-Kristensen, B., 2015. Altered knee joint neuromuscular control during landing from a jump in 10–15 year old children with Generalised Joint Hypermobility. A substudy of the CHAMPS-study Denmark. J. Electromyog. Kinesiol. 25 (3), 501–507.
Kiapour, A.M., Demetropoulos, C.K., Kiapour, A., Quatman, C.E., Wordeman, S.C., Goel, V.K., Hewett, T.E., 2016. Strain response of the anterior cruciate ligament to uniplanar and multiplanar loads during simulated landings: implications for injury mechanism. Am. J. Sports Med. 44 (8), 2087–2096.
King, E., Richter, C., Franklyn-Miller, A., Daniels, K., Wadey, R., Moran, R., Strike, S., 2018. Whole-body biomechanical differences between limbs exist 9 months after ACL reconstruction across jump/landing tasks. Scand. J. Med. Sci. Sports 28, 2567–2578.
Koga, H., Nakamae, A., Shima, Y., Iwasa, J., Myklebust, G., Engebretsen, L., Bahr, R., Krosshaug, T., 2010. Mechanisms for noncontact anterior cruciate ligament injuries: knee joint kinematics in 10 injury situations from female team handball and basketball. Am. J. Sports Med. 38 (11), 2218–2225.
Koo, T.K., Li, M.Y., 2016. A guideline of selecting and reporting intraclass correlation coefficients for reliability research. J. Chiropractic Med. 15 (2), 155–163.
Kotsifaki, A., Korakakis, V., Graham-Smith, P., Sideris, V., Whiteley, R., 2021. Vertical and horizontal hop performance: contributions of the hip, knee, and ankle. Sports Health 13 (2), 128–135. https://doi.org/10.1177/1941738120976363.
Kotsifaki, A., Korakakis, V., Whiteley, R., Van Rossom, S., Jonkers, I., 2020. Measuring only hop distance during single leg hop testing is insufficient to detect deficits in knee function after ACL reconstruction: a systematic review and meta-analysis. Br. J. Sports Med. 54 (3), 139–153.
Kristianslund, E., Krosshaug, T., van den Bogert, A.J., 2012. Effect of low pass filtering on joint moments from inverse dynamics: implications for injury prevention. J. Biomech. 45 (4), 666–671.
Krosshaug, T., Nakamae, A., Boden, B.P., Engebretsen, L., Smith, G., Slauterbeck, J.R., Hewett, T.E., Bahr, R., 2007. Mechanisms of anterior cruciate ligament injury in basketball: video analysis of 39 cases. Am. J. Sports Med. 35 (3), 359–367.
Logerstedt, D., Grindem, H., Lynch, A., Eitzen, I., Engebretsen, L., Risberg, M.A., Axe, M. J., Snyder-Mackler, L., 2012. Single-legged hop tests as predictors of self-reported knee function after anterior cruciate ligament reconstruction: the Delaware-Oslo ACL cohort study. Am. J. Sports Med. 40 (10), 2348–2356.
Markström, J.L., Grip, H., Schelin, L., Häger, C.K., 2019. Dynamic knee control and movement strategies in athletes and non-athletes in side hops: Implications for knee injury. Scand. J. Med. Sci. Sports 29 (8), 1181–1189.
Markström, J.L., Schelin, L., Häger, C.K., 2021. A novel standardised side hop test reliably evaluates landing mechanics for anterior cruciate ligament reconstructed persons and controls. Sports Biomech. 20 (2), 213–229.
Markström, J.L., Grip, H., Schelin, L., Häger, C.K., 2020. Individuals with an anterior cruciate ligament–reconstructed knee display atypical whole body movement strategies but normal knee robustness during side-hop landings: A finite helical axis analysis. Am. J. Sports Med. 48 (5), 1117–1126.
McGinley, J.L., Baker, R., Wolfe, R., Morris, M.E., 2009. The reliability of three-dimensional kinematic gait measurements: a systematic review. Gait Posture 29 (3), 360–369.
McGraw, K.O., Wong, S.P., 1996. Forming inferences about some intraclass correlation coefficients. Psychol. Methods 1 (1), 30–46.

Meng, L., Millar, L., Childs, C., Buis, A., 2020. A strathclyde cluster model for gait kinematic measurement using functional methods: a study of inter-assessor reliability analysis with comparison to anatomical models. Comp. Methods Biomech. Biomed. Engin. 23 (12), 844–853.
Milner, C.E., Westlake, C.G., Tate, J.J., 2011. Test–retest reliability of knee biomechanics during stop jump landings. J. Biomech. 44 (9), 1814–1816.
Mok, K.-M., Bahr, R., Krosshaug, T., 2018. Reliability of lower limb biomechanics in two sport-specific sidestep cutting tasks. Sports Biomech. 17 (2), 157–167.
Myer, G.D., Bates, N.A., DiCesare, C.A., Foss, K.D.B., Thomas, S.M., Wordeman, S.C., Sugimoto, D., Roewer, B.D., McKeon, J.M.M., Di Stasi, S.L., Noehren, B.W., McNally, M., Ford, K.R., Kiefer, A.W., Hewett, T.E., 2015. Reliability of 3-dimensional measures of single-leg drop landing across 3 institutions: implications for multicenter research for secondary ACL-injury prevention. J. Sport Rehabil. 24 (2), 198–209.
Paterno, M.V., Greenberger, H.B., 1996. The test-retest reliability of a one legged hop for distance in young adults with and without ACL reconstruction. Isokin. Exerc. Sci. 6 (1), 1–6.
Peebles, A.T., Miller, T.K., Queen, R.M., 2021. Landing biomechanics deficits in anterior cruciate ligament reconstruction patients can be assessed in a non-laboratory setting. J. Orthop. Res. https://doi.org/10.1002/jor.25039.
Pini, A., Markström, J.L., Schelin, L., 2019. Test-retest reliability measures for curve data: an overview with recommendations and supplementary code. Sports Biomech 1–22. https://doi.org/10.1080/14763141.2019.1655089.
R Core Team., 2019. R: A Language and Environment for Statistical Computing. R Foundation for Statistical Computing, Vienna, Austria https://www.R-project.org/.
Read, P.J., Oliver, J.L., De Ste Croix, M.B.A., Myer, G.D., Lloyd, R.S., 2018. A prospective investigation to evaluate risk factors for lower extremity injury risk in male youth soccer players. Scand. J. Med. Sci. Sports 28 (3), 1244–1251.
Roewer, B.D., Ford, K.R., Myer, G.D., Hewett, T.E., 2014. The 'impact' of force filtering cut-off frequency on the peak knee abduction moment during landing: artefact or 'artifiction'? Br. J. Sports Med. 48 (6), 464–468.
Røislien, J., Skare, Ø., Opheim, A., Rennie, L., 2012. Evaluating the properties of the coefficient of multiple correlation (cmc) for kinematic gait data. J. Biomech. 45 (11), 2014–2018.
Sado, N., Shiotani, H., Saeki, J., Kawakami, Y., 2021. Positional difference of malleoli-midpoint from three-dimensional geometric centre of rotation of ankle and its effect on ankle joint kinetics. Gait Posture 83, 223–229.
Saito, A., Okada, K., Sasaki, M., Wakasa, M., 2020. Influence of the trunk position on knee kinematics during the single-leg landing: implications for injury prevention. Sports Biomech. https://doi.org/10.1080/14763141.2019.1691642.
Sankey, S.P., Raja Azidin, R.M.F., Robinson, M.A., Malfait, B., Deschamps, K., Verschueren, S., Staes, F., Vanrenterghem, J., 2015. How reliable are knee kinematics and kinetics during side-cutting manoeuvres? Gait Posture 41 (4), 905–911.
Satterthwaite, F.E., 1946. An approximate distribution of estimates of variance components. Biometrics Bull. 2 (6), 110. https://doi.org/10.2307/3002019.
Schache, A.G., Baker, R., Lamoreux, L.W., 2006. Defining the knee joint flexion-extension axis for purposes of quantitative gait analysis: an evaluation of methods. Gait Posture 24 (1), 100–109.
Schwartz, M.H., Rozumalski, A., 2005. A new method for estimating joint parameters from motion data. J. Biomech. 38 (1), 107–116.
Schwartz, M.H., Trost, J.P., Wervey, R.A., 2004. Measurement and management of errors in quantitative gait data. Gait Posture 20 (2), 196–203.
Trevethan, R., 2017. Intraclass correlation coefficients: clearing the air, extending some cautions, and making some requests. Health Serv. Outcomes Res. Methodol. 17 (2), 127–143. https://doi.org/10.1007/s10742-016-0156-6.
van der Harst, J.J., Gokeler, A., Hof, A.L., 2007. Leg kinematics and kinetics in landing from a single-leg hop for distance. A comparison between dominant and non-dominant leg. Clin. Biomech. 22 (6), 674–680.
Warmenhoven, J., Cobley, S., Draper, C., Harrison, A., Bargary, N., Smith, R., 2019a. Bivariate functional principal components analysis: considerations for use with multivariate movement signatures in sports biomechanics. Sports Biomech. 18 (1), 10–27.
Warmenhoven, J., Cobley, S., Draper, C., Harrison, A., Bargary, N., Smith, R., 2019b. Considerations for the use of functional principal components analysis in sports biomechanics: Examples from on-water rowing. Sports Biomech. 18 (3), 317–341.
WEIR, JOSEPH.P., 2005. Quantifying test-retest reliability using the intraclass correlation coefficient and the sem. J. Strength Cond. Res. 19 (1), 231–240.
Wren, T.A.L., Mueske, N.M., Brophy, C.H., Pace, J.L., Katzel, M.J., Edison, B.R., Vandenberg, C.D., Zaslow, T.L., 2018. Hop distance symmetry does not indicate normal landing biomechanics in adolescent athletes with recent anterior cruciate ligament reconstruction. J. Orthop. Sports Phys. Ther. 48 (8), 622–629.